

# Synthesis of the CETP Inhibitor Torcetrapib: The Resolution Route and Origin of Stereoselectivity in the Iminium Ion Cyclization

David B. Damon,<sup>†</sup> Robert W. Dugger,<sup>\*,†,‡,⊥</sup> George Magnus-Aryitey,<sup>‡</sup> Roger B. Ruggeri,<sup>‡</sup> Ronald T. Wester,<sup>‡</sup> Meihua Tu,<sup>§</sup> and Yuriy Abramov<sup>\*,§,||</sup>

Chemical Research and Development, Department of Medicinal Chemistry, Exploratory Medicinal Chemistry, Pfizer Global Research and Development, Groton Labs, Eastern Point Road, Groton, Connecticut 06340, U.S.A.

## Abstract:

A practical, efficient synthesis of (–)-(2*R*,4*S*)-4-[(3,5-bis-trifluoromethyl-benzyl)methoxycarbonylamino]-2-ethyl-6-trifluoromethyl-3,4-dihydro-2*H*-quinoline-1-carboxylic acid ethyl ester (**1**), a cholesteryl ester transfer protein (CETP) inhibitor, is described. The key reaction in the synthesis, addition of an *N*-vinylcarbamate to an iminium ion rapidly followed by an iminium ion cyclization onto the aryl ring, sets up the *cis* relationship of the two substituents of the tetrahydroquinoline ring of **6**. The origin of the high *cis* stereoselectivity in the cyclization was explored using high-level quantum chemistry calculations.

## Introduction

Despite continuing advances in their understanding and treatment, cardiovascular diseases remain the leading cause of morbidity and mortality in the industrialized world. While most of the existing therapies in this area address the risk factors of hypertension and elevated low-density lipoprotein cholesterol (LDL-C), there remains a paucity of treatments for raising levels of high-density lipoprotein cholesterol (HDL-C). Pronounced elevation of HDL-C levels observed in subjects lacking a functional copy of the gene for cholesteryl ester transfer protein (CETP) offered strong evidence that an inhibitor of CETP might provide a therapy for raising low levels of HDL-C and the treatment of cardiovascular diseases. Torcetrapib (**1**, CP-529,414) is an inhibitor of CETP that is currently being developed for the treatment of atherosclerosis and coronary heart disease. The success of this program required a practical method for preparing torcetrapib on a large scale in a reliable manner. Synthetic routes used to prepare materials to support the clinical development of torcetrapib are described in this article<sup>1</sup> and in the following article.<sup>2</sup>

\* To whom correspondence should be addressed. E-mail: robert.w.dugger@pfizer.com, yuriy.a.abramov@pfizer.com.

<sup>⊥</sup> Correspondence regarding the synthetic aspects of this paper should be directed to R. Dugger (robert.w.dugger@pfizer.com).

<sup>||</sup> Correspondence regarding the computational aspects of this paper should be directed to Y. Abramov (yuriy.a.abramov@pfizer.com).

<sup>†</sup> Chemical Research and Development.

<sup>‡</sup> Department of Medicinal Chemistry.

<sup>§</sup> Exploratory Medicinal Chemistry.

(1) See Damon, D. B.; Dugger, R. W. Eur. Pat. Appl. EP1125929, Aug. 22, 2001 and U.S. Patent 6,313,142, Nov. 6, 2001 for the original disclosure of this work.

(2) Damon, D. B.; Dugger, R. W.; Hubbs, S. E.; Scott, J. M.; Scott, R. W. *Org. Process Res. Dev.* **2006**, *10*, 472 (the following article in this issue).

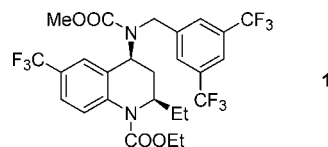
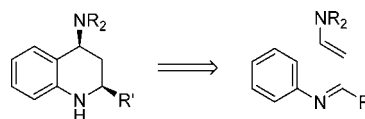


Figure 1. Structure of torcetrapib (CP-529,414).

## Scheme 1



## Results and Discussion

**Synthesis.** Key to the synthesis of **1** is the construction of the tetrahydroquinoline nucleus with the *cis* stereochemistry of the substituents. The aza Diels–Alder reaction of *N*-arylimines and *N*-vinyl compounds (Scheme 1) seemed ideal since it is often associated with a high degree of *cis* selectivity.<sup>3</sup>

Imine **3** (Scheme 2) was generated in situ in CH<sub>2</sub>Cl<sub>2</sub> from *p*-trifluoromethylaniline<sup>4</sup> and *n*-propanal using TiCl<sub>4</sub> as a water scavenger. Addition of vinyl carbamate **5**<sup>5</sup> and catalytic amounts of BF<sub>3</sub>·OEt<sub>2</sub> produced **6** with no detectable amount of the *trans* isomer (by NMR); however, the yield was low (40–60%), and the purity of the product was modest (~70%). After several attempts at improving the yield by varying conditions it became clear to us that imine **3** was not being formed cleanly; significant amounts of amina **4** were also formed, thus leading to the low yields and low purity.

Since imine **3** seemed to be unstable towards further additions, we sought to trap **3** with a nucleophile that could subsequently regenerate the imine in situ in the next step. The variation reported by Katritzky<sup>6</sup> in which the imine is trapped as its benzotriazole adduct seemed ideal. In Katritzky's work, the *cis* isomer was also the only stereoisomer observed.

In our hands, stirring aniline **2** with *n*-propanal and benzotriazole in toluene followed by addition of *n*-heptane

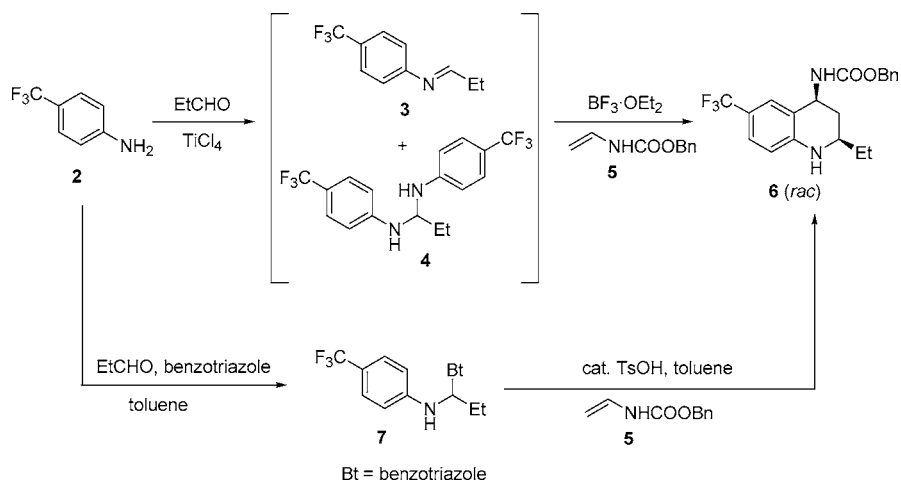
(3) (a) Crousse, B.; Bégué, J.; Bonnet-Delpon, D. *J. Org. Chem.* **2000**, *65*, 5009. (b) Stevenson, G.; Leeson, P.; Rowley, M.; Sanderson, I.; Stansfield, I. *Bioorg. Med. Chem. Lett.* **1992**, *2*, 371.

(4) Hazards associated with the storage of *p*-trifluoromethylaniline have been described. Users of this compound are urged to take the appropriate precautions. See Tickner, D.; Kasthurikrishnan, N. *Org. Process Res. Dev.* **2001**, *5*, 270.

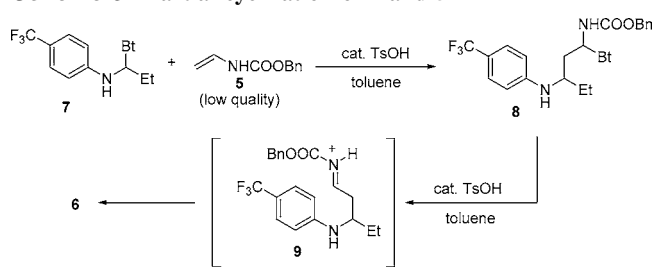
(5) am Ende, D. J.; DeVries, K. M.; Clifford, P. J.; Brenek, S. J. *Org. Process Res. Dev.* **1998**, *2*, 382.

(6) Katritzky, A. R.; Rachwal, B.; Rachwal, S. *J. Org. Chem.* **1995**, *60*, 3993.

## Scheme 2



## Scheme 3. Partial cyclization of 7 and 5



resulted in **7** crystallizing from the reaction mixture in 91% yield (two crops). With a crystalline imine surrogate in hand, we next investigated its reaction with vinyl carbamate **5**. Treating a toluene solution of **7** and **5** with 1 mol % toluenesulfonic acid resulted in a 78% yield of **6**. Again, no trans isomer was detectable. This method of producing **6** also has the advantage of not requiring the use of the moisture-sensitive Lewis acids,  $\text{TiCl}_4$  and  $\text{BF}_3 \cdot \text{OEt}_2$ .

Interestingly, in one run using a low-quality batch of **5** we observed the formation of a large amount of a byproduct (Scheme 3). The byproduct was isolated and shown to be **8** (a 1:1 mixture of diastereomers). Resubjecting **8** to the standard cyclization conditions provided **6** in excellent yield (92%). Again, only the cis isomer was observed. This observation is consistent with the stepwise process reported by Katritzky.<sup>6</sup>

Acylation of **6** (Scheme 4) is difficult due to steric hindrance of the adjacent ethyl group and the low nucleophilicity of the aniline nitrogen due to the electron-withdrawing effect of the *p*-trifluoromethyl group. A variety of reaction conditions were investigated to find the optimum conditions. Pyridine was found to be the best base. The best yield of **10** was obtained when an excess of ethyl chloroformate (5 equiv) was slowly added to the reaction mixture over a period of 4 h. Aqueous workup followed by crystallization provided **10** in 83% yield. Although multigram quantities of **10** could be separated into its enantiomers via chiral chromatography, for the quantities we needed for development of this candidate we felt that a classical resolution would be more expedient. Amine **11** was prepared in excellent yield (93%) by hydrogenolysis of the benzyl-carbamate protecting group of **10** under transfer hydro-

genolysis conditions using ammonium formate as the reducing agent.<sup>7</sup> We screened numerous chiral acids to find a suitable salt for resolution of **11**. Dibenzoyl-L-tartrate was the best lead identified from our initial screen. Aqueous ethanol was identified as the optimal solvent system. Using 3% water (w/w) gave the best results, a salt of 98% de in 39% yield (78% of theory). NMR integration of the salt indicated that it was a hemi-tartrate salt (2 equiv of amine per tartrate). The structure and absolute stereochemistry of **12** were confirmed by an X-ray crystallographic structure determination.<sup>8</sup>

Breaking the salt and isolation of the free amine were often accompanied by the formation of byproducts. Fortunately, we found that isolation of the free amine was unnecessary. Slurrying salt **12** in dichloroethane and treating with aqueous NaOH produced a dichloroethane solution of the free base that could be dried and carried directly into the reductive amination reaction. Adding aldehyde **13** and sodium triacetoxyborohydride<sup>9</sup> to the dichloroethane solution resulted in conversion to desired benzylamine **14**. We found it convenient to isolate the product of the reductive amination as the toluenesulfonate salt by dissolving the crude free base in a mixture of methanol and diisopropyl ether and adding toluenesulfonic acid. This process provided **14** in 86% yield from **12**. Installing the final carbamate by treating **14** with methylchloroformate in THF with  $\text{Na}_2\text{CO}_3$  as the base to neutralize the toluenesulfonic acid and HCl produced **1** in high yield. The final product is very soluble in most organic solvents but can be crystallized from concentrated ethanol solutions as the monoethanolate in 74% yield.

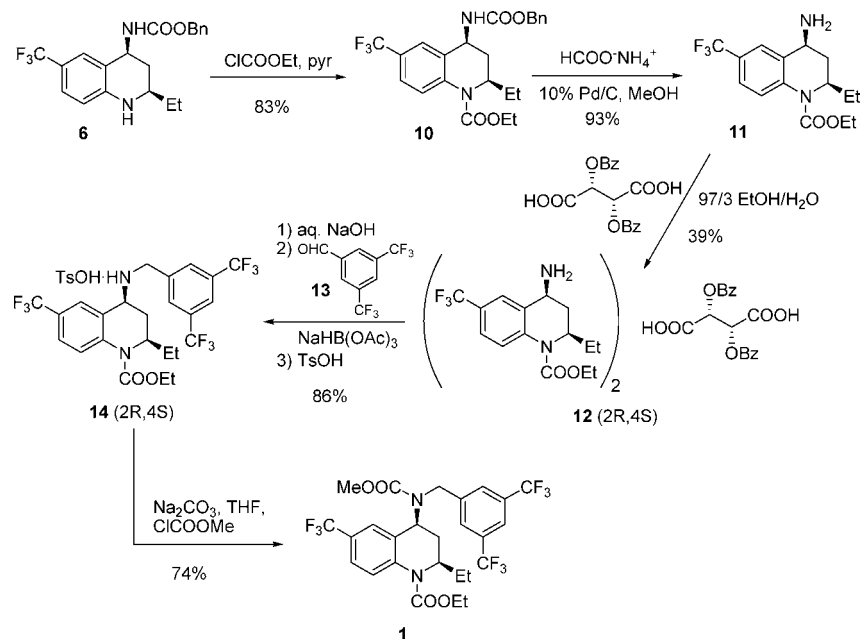
**Origin of the Stereoselectivity.** Although high cis selectivity is preceded in the literature,<sup>3,4</sup> it seemed unusual that we could detect no trans isomer at all, and so it was decided to utilize molecular modeling to gain a better understanding of this process. High-level quantum chemistry calculations were adopted to rationalize the cis selectivity in the cyclization of the activated iminium ion **9**. For

(7) Johnstone, R. A. W.; Wilby, A. H.; Entwistle, I. D. *Chem. Rev.* **1985**, *85*, 129.

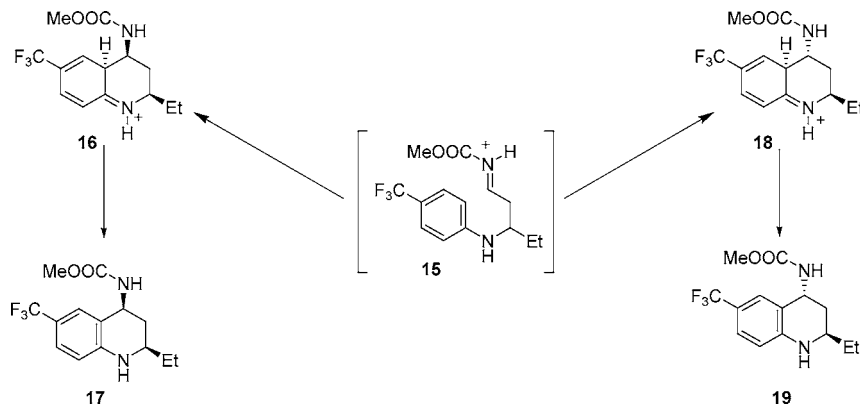
(8) Details can be found in the Supporting Information.

(9) Abdel-Magid, A. F.; Maryanoff, C. A.; Carson, K. G. *Tetrahedron. Lett.* **1990**, *31*, 5595.

Scheme 4



Scheme 5. Cyclization pathways to cis and trans products



simplicity, the methyl carbamate **15** was modeled instead of the benzyl carbamate (Scheme 5).

Stereoselectivity, as a general phenomenon, arises from free energy differences associated with diastereomeric transition states (kinetic control) or products (thermodynamic control). There are four possible diastereomers of the intermediate cyclization products of **15**, two cis and two trans. Only two of them, **16** and **18**, were found to have the lowest energies and became the focus of further modeling. The calculated relative energy difference for those diastereomers, as well as for the corresponding final products, **17** and **19**, appeared to be  $-0.8$  and  $-0.3$  kcal/mol, respectively. Since these results do not account for the observed high stereoselectivity, the kinetic consideration was pursued. For this, the formation of the intermediate cyclization products, **16** and **18**, was assumed to be a rate-limiting step.

The three lowest-energy conformations of **15** (reactant conformers, RC) are shown in Figure 2. Among those, RC1 and RC3 are precursors for the respective cis and trans cyclization. The corresponding transition state (TS) geometries for cyclization,  $TS_{cis}$  and  $TS_{trans}$ , are shown in Figure 3. Conformations RC1 and RC3 and products **16** and **18**

present a Curtin-Hammet kinetic system, in which a reactant exists in two interconverting forms, each of which give different products.<sup>10</sup> To evaluate a product ratio for such a system, a consideration of both reaction kinetics and kinetics of the conformational interconversion should be performed.

The cyclization and conformational pathways are presented in Figure 4a,b. According to MP2 calculations, the RC1 conformer is the global minimum of the potential surface area and is separated from RC3 by 3.0 kcal/mol. The energy difference increases up to 4.4 kcal/mol for the cis and trans cyclization transition states. At the same time, the absolute values of the activation energies appear to be very low, especially for the cis cyclization. This result is a likely consequence of the implicit solvation model (using the nonionic solvent, DMSO), which underestimates the electrostatic stabilization of the cation, **15**, by a counterion. The stabilization is less favorable for the reaction transition states than for the RC1 and RC3 conformers, since the cationic charge becomes more diffused as a result of a partial charge transfer (of about  $0.16 e^-$  for both  $TS_{cis}$  and  $TS_{trans}$ ) be-

(10) Seeman, J. I. *Chem. Rev.* **1983**, *83*, 83.

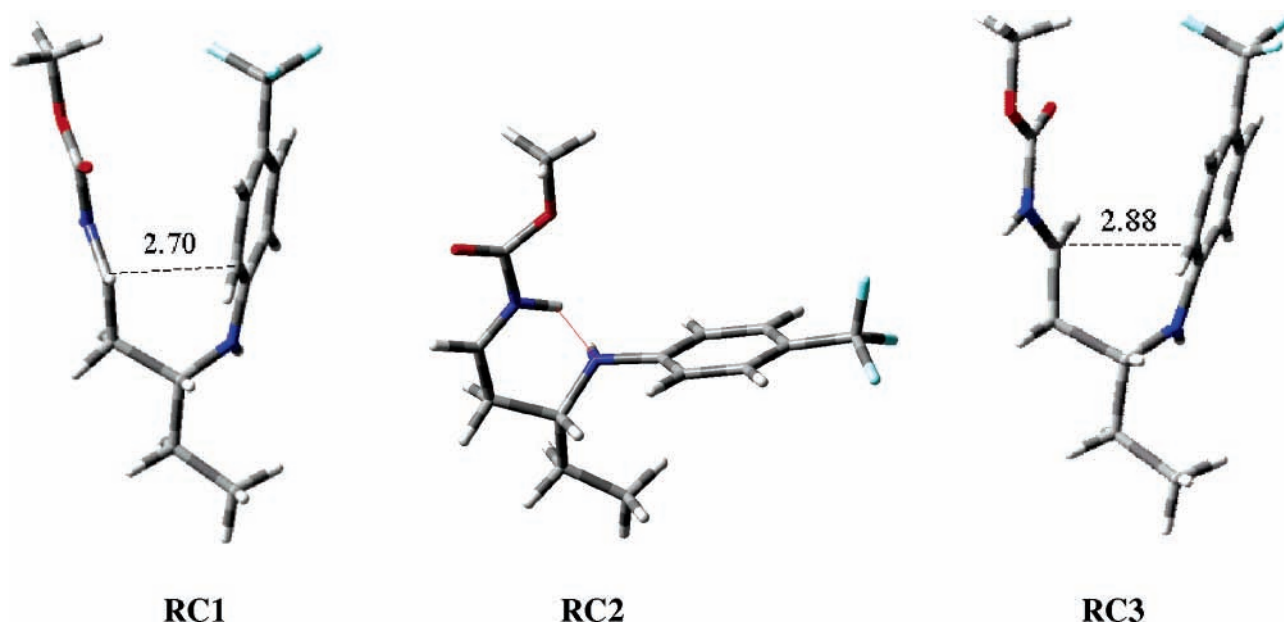


**Figure 2.** Lowest-energy conformers of 15. RC1 and RC3 are precursors for respectively cis and trans cyclization. Distances between atoms closing the ring are indicated in Å.

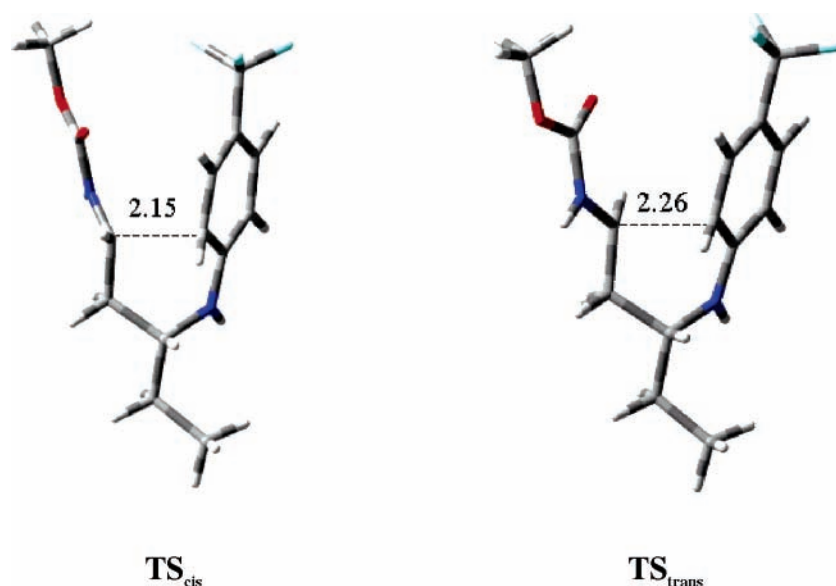


**Figure 3.** Transition-state geometries for the cis and trans cyclization. Distances between atoms closing the ring are indicated in Å.

tween nucleophilic (trifluoromethylaniline) and electrophilic (iminium side chain) fragments of the molecule. As a result, the reaction activation barriers should increase by approximately an equal amount. To verify this consideration, a simplified model study was performed. Each of the RC1, RC3, TS<sub>cis</sub>, and TS<sub>trans</sub> structures was explicitly solvated by one Cl<sup>-</sup> counterion, displaying a close contact with the H(N) hydrogen of the iminium cation. For this purpose, only counterion positions were optimized, while keeping the molecule rigid. This was followed by a single-point implicit solvation of the neutral complex in toluene. The resulting energy differences between the “ground” and “transition” states were compared with the corresponding values obtained at the same level of theory and adopting implicit DMSO solvation with no counterion consideration. The estimated increase of the activation energies for the trans and cis

cyclization, due to the counterion stabilization, was respectively 2.5 and 3.4 kcal/mol (3.6 and 4.4 kcal/mol in gas phase). The estimated change of the energy difference between the reaction transition states was 0.2 kcal/mol.

TS<sub>31</sub> displays the lowest barrier along the conformational pathway between RC1 and RC3 (Figure 4b). The resulting activation energies for the direct and reverse interconversion between the conformers are 5.2 kcal/mol and 2.2 kcal/mol, respectively. The latter energy is comparable with the trans cyclization activation barrier of 1.9 kcal/mol, without any adjustment on the counterion effect. However, the atomic charge analysis of the TS<sub>31</sub> reflects its higher polarity relative to that of the RC1 and RC3 conformers: the charge separation between nucleophilic and electrophilic fragments is about 0.12 e<sup>-</sup> higher. As a result, an additional stabilization of this transition state and a lowering of the interconversion

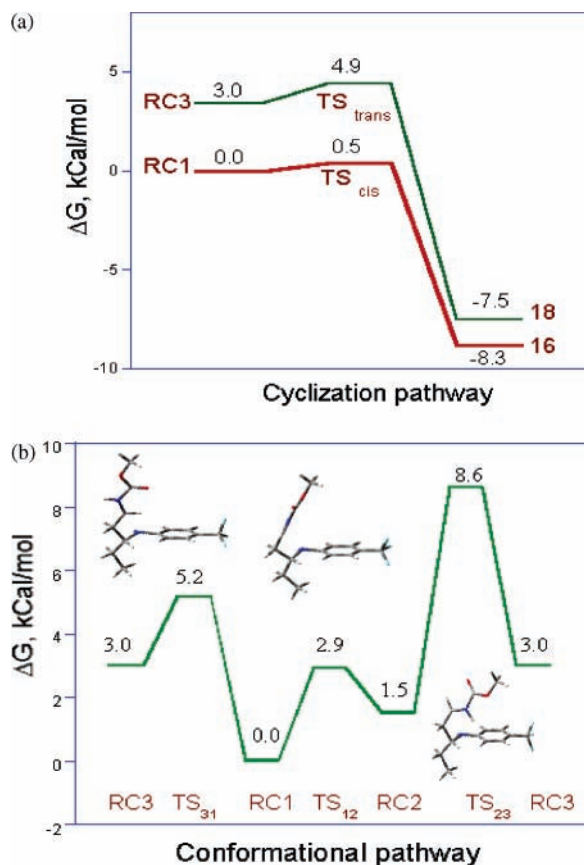


**Figure 4.** Potential energy profile of **15**: (a) cyclization pathway; (b) conformational pathway.

barrier between RC3 and RC1 should take place due to the electrostatic interaction with the counterion in solution.

On the basis of the above considerations, we assume that the interconversion between the reactant conformers, RC1 and RC3, takes place faster (a lower barrier) than cyclization towards the cis and trans products (higher barriers). In that case, the cis-to-trans product ratio can be described by the Arrhenius equation:  $\text{cis/trans} = e^{-(\Delta G(\text{TS}_{\text{cis}}) - \Delta G(\text{TS}_{\text{trans}}))/RT}$ . The predicted energy difference of 4.4 kcal/mol accounts for the cis stereoselectivity of more than 99.9%. Therefore, the origin of the stereoselectivity takes place from a noticeably more stable reactant conformer and the lower activation energy for the cis cyclization.

The cyclization reaction can be also qualitatively rationalized in terms of frontier molecular orbital (FMO) theory.<sup>11</sup> Within this approach, the reaction is driven by the favorable interaction between the highest occupied (HOMO) and the lowest unoccupied (LUMO) molecular orbitals of the respectively nucleophilic and electrophilic species. The frontier orbitals of **15** are predominately located at the phenyl (HOMO) and carbamate fragments (LUMO), displaying maximum constructive overlap along the reaction path (Figure 5). An intramolecular mixing of these orbitals during the cyclization leads to electronic stabilization of the transition state; this is due to lowering the HOMO and raising the LUMO energies. The net effect, at the PCM-B3LYP/6-31+G(d,p) level of theory in DMSO, is an increase of the

HOMO–LUMO gap from 3.20 eV, for the RC1, to 3.75 eV, for  $\text{TS}_{\text{cis}}$ .

In terms of the FMO theory, the observed stereoselectivity may be rationalized as a result of the more favorable secondary interaction between LUMO, at the N–C $\alpha$  bond of the carbamate, and HOMO, at the C4–C3 bond of the phenyl ring: the difference between N–C4 distances of the  $\text{TS}_{\text{trans}}$  and  $\text{TS}_{\text{cis}}$  transition states is 0.8 Å.

## Conclusion

The route we developed to prepare **1** proceeds in 13.5% overall yield over seven steps from *p*-trifluoromethylaniline. It has been scaled several times to produce multikilogram quantities needed for the development of this exciting drug candidate. Although this process was suitable for early development purposes, a better route was needed for larger-scale manufacture. Investigations towards an improved route are described in the following paper. The origin of the high cis stereoselectivity in the cyclization was rationalized by high-level quantum chemistry calculations. It was demonstrated that the selectivity is kinetically controlled, originating from both the ground-state conformational preference and from the lower activation energy of the cis cyclization.

## Computational Section

The origin of cis stereoselectivity of the cyclization product of **15** (Scheme 5) was investigated by means of quantum chemical calculations performed with the Gaussian03 program.<sup>12</sup> Initial conformational search for **15** and cyclization products **16**, **17**, **18**, and **19** was performed using the Monte Carlo Multiple Minimum (MCM) method, adopting MMF94s force field with GBSA solvation as implemented in MacroModel.<sup>13</sup> It was followed by gas-phase geometry optimization at the B3LYP/6-31G(d) level of theory.<sup>14</sup> Transition states were calculated at the same level of theory using a quadratic synchronous transit algorithm (STQN).<sup>15</sup> The nature of all stationary points was confirmed by the frequency calculations. GaussView 3.09<sup>16</sup> was used to animate the imaginary frequencies of the TS structures; this was done to confirm that the displacement vectors are placed

(12) Frisch, M. J.; Trucks, G. W.; Schlegel, H. B.; Scuseria, G. E.; Robb, M. A.; Cheeseman, J. R.; Montgomery, J. A., Jr.; Vreven, T.; Kudin, K. N.; Burant, J. C.; Millam, J. M.; Iyengar, S. S.; Tomasi, J.; Barone, V.; Mennucci, B.; Cossi, M.; Scalmani, G.; Rega, N.; Petersson, G. A.; Nakatsuji, H.; Hada, M.; Ehara, M.; Toyota, K.; Fukuda, R.; Hasegawa, J.; Ishida, M.; Nakajima, T.; Honda, Y.; Kitao, O.; Nakai, H.; Klene, M.; Li, X.; Knox, J. E.; Hratchian, H. P.; Cross, J. B.; Bakken, V.; Adamo, C.; Jaramillo, J.; Gomperts, R.; Stratmann, R. E.; Yazyev, O.; Austin, A. J.; Cammi, R.; Pomelli, C.; Ochterski, J. W.; Ayala, P. Y.; Morokuma, K.; Voth, G. A.; Salvador, P.; Dannenberg, J. J.; Zakrzewski, V. G.; Dapprich, S.; Daniels, A. D.; Strain, M. C.; Farkas, O.; Malick, D. K.; Rabuck, A. D.; Raghavachari, K.; Foresman, J. B.; Ortiz, J. V.; Cui, Q.; Baboul, A. G.; Clifford, S.; Cioslowski, J.; Stefanov, B. B.; Liu, G.; Liashenko, A.; Piskorz, P.; Komaromi, I.; Martin, R. L.; Fox, D. J.; Keith, T.; Al-Laham, M. A.; Peng, C. Y.; Nanayakkara, A.; Challacombe, M.; Gill, P. M. W.; Johnson, B.; Chen, W.; Wong, M. W.; Gonzalez, C.; Pople, J. A. *Gaussian 03*, Revision B.04; Gaussian, Inc.: Wallingford CT, 2004.

(13) *MacroModel*; Schrodinger Inc.: Portland, OR

(14) (a) Becke, A. D. *J. Chem. Phys.* **1993**, *98*, 5648. (b) Lee, C.; Yang, W.; Parr, R. G. *Phys. Rev. B* **1988**, *37*, 785. (c) Hariharan, P. C., Pople J. A. *Theor. Chim. Acta* **1973**, *28*, 213.

(15) (a) Peng, C.; Ayala, P. Y.; Schlegel, H. B.; Frisch, M. J. *J. Comput. Chem.* **1996**, *17*, 49. (b) Peng, C.; Schlegel, H. B. *Isr. J. Chem.* **1994**, *33*, 449.

(16) *GaussView*, rev. 3.0, Semichem, Inc. for Gaussian, Inc. 1998.

(11) Fukui, K. *Acc. Chem. Res.* **1981**, *14*, 363.

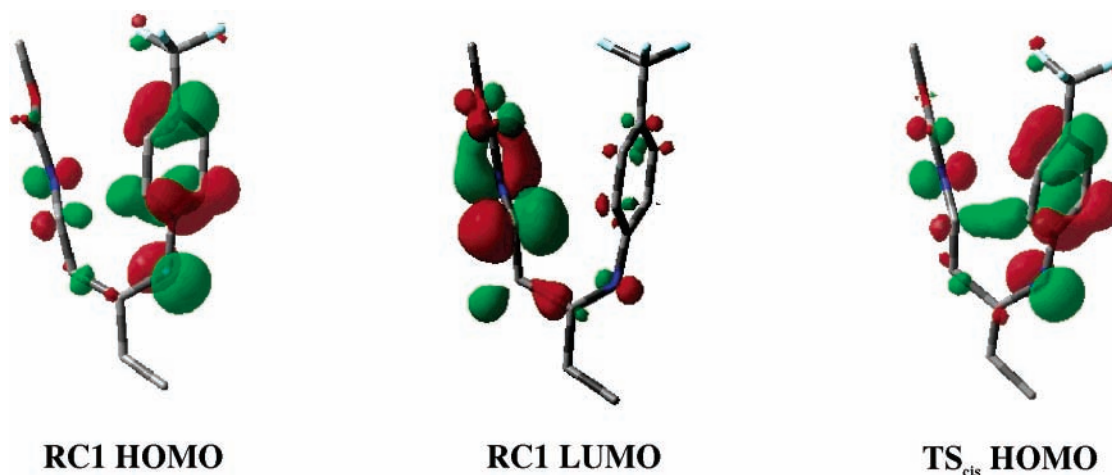


**Figure 5.** Frontier orbital analysis of the *cis* cyclization. The  $\pm 0.05$  au isosurfaces of the orbitals are shown.

along the reaction coordinates. Finally, the reported free energies at the zero temperature were calculated at the optimized geometries as:  $\Delta G = E_{el} + ZPE + \Delta G_{sol}$ . The electronic energies,  $E_{el}$ , were obtained by the single-point MP2/6-31+G(d,p)<sup>17</sup> calculations in gas phase. Zero-point energy (ZPE) corrections at the B3LYP/6-31G(d) level were scaled by a factor of 0.9806.<sup>18</sup> The solvation free energies,  $\Delta G_{sol}$ , were calculated in DMSO and in toluene, using the PCM model<sup>19</sup> at the B3LYP/6-31+G(d) level of theory, adopting UAKS atomic radii.<sup>20</sup> Modeling of the salt bridge with Cl<sup>-</sup> anion was performed at the B3LYP/6-31+G(d)//B3LYP/3-21G(d) level of theory. The atomic charges were estimated according to the Mulliken population.

### Experimental Section

All materials were purchased from commercial suppliers and used without further purification. All reactions were conducted under an atmosphere of nitrogen unless noted otherwise. <sup>1</sup>H and <sup>13</sup>C-spectroscopy was performed at 300 and 400 MHz on Bruker-Spectrospin Avance instruments.

**(1-Benzotriazol-1-yl-propyl)-(4-trifluoromethyl-phenyl)-amine (7).** A 2-L flask under nitrogen atmosphere was charged with benzotriazole (36.96 g, 310 mmol, 1.0 equiv) and dry toluene (400 mL). A room-temperature solution of *p*-trifluoromethylaniline<sup>4</sup> (39.1 mL, 310 mmol, 1.0 equiv) and 50 mL of toluene was added over 1 min. A room-temperature solution of *n*-propanal (24.6 mL, 341 mmol, 1.1 equiv) and 50 mL of toluene was then added over 20 min. There was an exotherm from 23 to 30 °C during this addition. After stirring 24 h, *n*-heptane (500 mL) was added, and the slurry stirred an additional 1 h. The suspension was filtered, and the solids were washed with *n*-heptane (1 × 100 mL and then 1 × 200 mL) and were dried. **7** was isolated as shiny white needles (81.3 g, 82%). After 24 h, a second crop was isolated from the filtrate (8.7 g, 9%). mp 130–132 °C; <sup>1</sup>H NMR (DMSO-*d*<sub>6</sub>, 400 MHz)  $\delta$  0.82 (t, 3H,  $J = 7.5$  Hz),

2.25 (m, 2H), 6.49 (m, 1H), 6.80 (d, 2H,  $J = 8.7$  Hz), 7.35 (m, 3H), 7.50 (m, 1H), 7.88 (d, 1H,  $J = 8.3$  Hz), 7.99 (m, 1H), 8.09 (d, 1H,  $J = 8.5$  Hz), none of the N-2 benzotriazole isomer was observed;<sup>6</sup> <sup>13</sup>C NMR (DMSO-*d*<sub>6</sub>, 100 MHz)  $\delta$  149.3, 146.1, 131.4, 127.7, 126.8, 125.3 (q,  $J = 270$  Hz), 124.4, 119.8, 118.2 (q,  $J = 31.7$  Hz), 112.9, 111.5, 71.0, 28.0, 10.2; DEPT spectrum: quaternary carbons  $\delta$  149.3, 146.1, 131.4, 125.3, 118.2; CH carbons  $\delta$  127.7, 126.8, 124.4, 119.8, 112.9, 111.5, 71.0; CH<sub>2</sub> carbon  $\delta$  28.0; CH<sub>3</sub> carbon  $\delta$  10.2; IR (drifts) 3292 (s), 3038 (m), 2975 (m), 1621 (s), 1331 (s), 1320 (s), 1114 (vs); Anal. Calcd for C<sub>16</sub>H<sub>15</sub>N<sub>4</sub>F<sub>3</sub>: C, 59.99; H, 4.72; N, 17.49. Found (first crop): C, 60.16; H, 4.74; N, 17.86. Found (second crop): C, 59.97; H, 4.66; N, 17.63.

**cis-(2-Ethyl-6-trifluoromethyl-1,2,3,4-tetrahydro-quinolin-4-yl)carbamic Acid Benzyl Ester (6).** To a 1-L flask under nitrogen atmosphere charged with **5** (27.66 g, 156 mmol, 1.0 equiv) were added dry toluene (500 mL), **7** (50.0 g, 156 mmol, 1.0 equiv), and *p*-toluenesulfonic acid monohydrate (297 mg, 1.56 mmol, 0.01 equiv). The mixture was heated to 70 °C. After 2 h, the mixture was cooled to room temperature and transferred to a separatory funnel. Ethyl acetate (500 mL) was added. The mixture was washed 1 × 200 mL of 1 N NaOH, 1 × 200 mL of H<sub>2</sub>O, 1 × 200 mL of brine, and dried (MgSO<sub>4</sub>). The mixture was filtered, and the solids were washed 1 × 50 mL of ethyl acetate. The filtrate was concentrated to ~250 mL; 500 mL of toluene was added, and the mixture was concentrated to ~500 mL. Five hundred milliliters of *n*-heptane was added, the slurry was stirred 1 h and filtered through a Buchner funnel and dried. **6** was isolated as a white powder (45.04 g, 76%): mp 155–157 °C; <sup>1</sup>H NMR (DMSO-*d*<sub>6</sub>, 400 MHz)  $\delta$  0.92 (t, 3H,  $J = 7.5$  Hz), 1.5 (m, 3H), 2.00 (m, 1H), 3.35 (m, 1H), 4.77 (m, 1H), 5.07 (d, 1H,  $J = 12.5$  Hz), 5.15 (d, 1H,  $J = 12.5$  Hz), 6.35 (s, 1H), 6.61 (d, 1H,  $J = 8.5$  Hz), 7.12 (s, 1H), 7.18 (dd, 1H,  $J = 1.9, 8.5$  Hz), 7.4 (m, 5H), 7.70 (d, 1H,  $J = 9.1$  Hz); <sup>13</sup>C NMR (DMSO-*d*<sub>6</sub>, 100 MHz)  $\delta$  157.03, 149.02, 137.79, 128.82, 128.23, 128.03, 125.9 (q,  $J = 270$  Hz), 125.0, 123.5, 121.7, 115.2 (q,  $J = 31.7$  Hz), 113.3, 65.8, 52.0, 47.8, 34.0, 28.6, 9.9; DEPT spectrum: quaternary carbons  $\delta$  157.0, 149.0, 137.7, 125.9, 121.7, 115.2; CH carbons  $\delta$  128.8, 128.2,

(17) (a) Møller, C.; Plesset, M. S. *Phys. Rev.* **1934**, *46*, 618. (b) Frisch, M. J.; Head-Gordon, M.; Pople, J. A. *Chem. Phys. Lett.* **1990**, *166*, 275.

(18) Scott, A. P.; Radom, L. *J. Phys. Chem.* **1996**, *100*, 16502.

(19) (a) Cossi, M.; Scalmani, G.; Rega, N.; Barone, V. *J. Chem. Phys.* **2002**, *117*, 43. (b) Cancès, E.; Mennucci, B.; Tomasi, J. *J. Chem. Phys.* **1997**, *107*, 3032.

(20) Barone, V.; Cossi, M.; Tomasi, J. *J. Chem. Phys.* **1997**, *107*, 3210.

128.0, 125.0, 123.5, 113.3, 52.0, 47.8; CH<sub>2</sub> carbons  $\delta$  65.8, 34.0, 28.6; CH<sub>3</sub> carbon  $\delta$  9.9; IR (drifts) 3430 (m), 3303 (s), 2951 (m), 1686 (vs), 1542 (vs), 1088 (vs); MS (APCI+) *m/z* (rel intens) 379 (M + H<sup>+</sup>, 53), 228 (100); Anal. Calcd for C<sub>20</sub>H<sub>21</sub>N<sub>2</sub>O<sub>2</sub>F<sub>3</sub>: C, 63.48; H, 5.59; N, 7.40; Found: C, 63.69; H, 6.06, N, 7.36.

**cis-4-Benzoyloxycarbonylamino-2-ethyl-6-trifluoromethyl-3,4-dihydro-2H-quinoline-1-carboxylic Acid Ethyl Ester (10).** A 3-L flask under nitrogen atmosphere was charged with **6** (96.0 g, 254 mmol, 1.0 equiv), dry dichloromethane (720 mL), and dry pyridine (103 mL, 1.27 mol, 5.0 equiv). A solution of ethyl chloroformate (121 mL, 1.27 mol, 5.0 equiv), in dry dichloromethane (240 mL), was added slowly over 4 h. The addition was exothermic and required a reflux condenser. Once the chloroformate addition was complete, the reaction was cooled in an ice bath and 1350 mL of 1 N NaOH was added. The mixture was stirred 15 min and then transferred to a separatory funnel. The layers were separated, and the aqueous was extracted 1  $\times$  1 L of dichloromethane. The combined dichloromethane layers were washed 1  $\times$  1350 mL of 1 N HCl, 1  $\times$  1 L of saturated aq NaHCO<sub>3</sub>, 1  $\times$  1 L of brine, and dried (Na<sub>2</sub>SO<sub>4</sub>). The mixture was filtered, and the filtrate concentrated to an orange oil. Five hundred and seventy milliliters of abs. ethanol was added, and the solution was concentrated. The solids were dissolved in 1370 mL of abs. ethanol, and 570 mL of H<sub>2</sub>O were added dropwise over 45 min. The resultant thick slurry stirred 18 h and filtered. The solids were washed with cold 7:3 abs. ethanol/water (1  $\times$  250 mL, then 1  $\times$  100 mL) and dried (vac oven, 45 °C) to give **10** as a white, crystalline solid (94.54 g, 83%): mp 92–96 °C; <sup>1</sup>H NMR (CDCl<sub>3</sub>, 400 MHz)  $\delta$  0.84 (t, 3H, *J* = 7.4 Hz), 1.28 (t, 3H, *J* = 7.0 Hz), 1.4 (m, 2H), 1.62 (m, 1H), 2.53 (m, 1H), 4.23 (m, 2H), 4.47 (m, 1H), 4.79 (m, 1H), 5.01 (d, 1H, *J* = 9.2 Hz), 5.18 (m, 2H), 7.4 (m, 5H), 7.5 (m, 2H), 7.57 (m, 1H); <sup>13</sup>C NMR (CDCl<sub>3</sub>, 100 MHz)  $\delta$  155.9, 154.4, 139.4, 136.2, 134.3, 128.6, 128.3, 128.2, 126.3 (q, *J* = 31.7 Hz), 126.1, 124.2, 124.19, 124.12 (q, *J* = 27.3 Hz), 120.74, 120.70, 67.2, 62.2, 53.4, 46.7, 37.7, 28.2, 14.3, 9.7; DEPT spectrum: quaternary carbons  $\delta$  155.9, 154.4, 139.4, 136.2, 134.3, 126.3, 124.12; CH carbons  $\delta$  128.6, 128.3, 128.2, 126.1, 124.22, 124.19, 120.74, 120.70, 53.4, 46.7; CH<sub>2</sub> carbons  $\delta$  67.2, 62.2, 37.7, 28.2; CH<sub>3</sub> carbons  $\delta$  14.3, 9.7; IR (drifts) 3304 (s), 3067 (m), 3033 (m), 2982 (m), 2932 (m), 1723 (s), 1693 (s), 1545 (s); MS (APCI+) *m/z* (rel intens) 451 (M + H<sup>+</sup>, 2), 300 (100); Anal. Calcd for C<sub>23</sub>H<sub>25</sub>N<sub>2</sub>O<sub>4</sub>F<sub>3</sub>: C, 61.33; H, 5.60; N, 6.22. Found: C, 61.07; H, 5.69; N, 6.22.

**cis-4-Amino-2-ethyl-6-trifluoromethyl-3,4-dihydro-2H-quinoline-1-carboxylic Acid Ethyl Ester (11).** A 1-L, four-neck flask under nitrogen atmosphere was charged with **10** (40.1 g, 89 mmol, 1.0 equiv), methanol (400 mL), and ammonium formate (14.0 g, 223 mmol, 2.5 equiv). To the slurry was added 10% Pd/C, 50% water wet (4.0 g), and the slurry was heated to 40 °C over 1 h. After 1.5 h, the mixture was cooled to room temperature and filtered through Celite. The cake was washed 2  $\times$  100 mL of methanol. The filtrate was concentrated to  $\sim$ 75 mL, transferred to a separatory funnel, and diluted with 400 mL of ethyl acetate. The mixture

was washed 1  $\times$  125 mL of saturated aq. NaHCO<sub>3</sub> and 1  $\times$  100 mL of brine, and dried (Na<sub>2</sub>SO<sub>4</sub>). The mixture was filtered and the filtrate concentrated to a clear oil. The oil was crystallized from 100 mL of *n*-heptane to give **11** as a white crystalline solid (26.05 g, 93%): mp 61.5–63.5 °C; <sup>1</sup>H NMR (CDCl<sub>3</sub>, 400 MHz)  $\delta$  0.79 (t, 3H, *J* = 7.5 Hz), 1.24 (m, 4H), 1.42 (m, 1H), 1.51 (br s, 2H), 1.62 (m, 1H), 2.46 (m, 1H), 3.73 (m, 1H), 4.17 (m, 2H), 4.36 (m, 1H), 7.44 (m, 2H), 7.66 (m, 1H); <sup>13</sup>C NMR (CDCl<sub>3</sub>, 100 MHz)  $\delta$  154.6, 139.3, 138.9, 126.3 (q, *J* = 32 Hz), 125.7, 124.3 (q, *J* = 27.1 Hz), 123.5, 119.8, 61.6, 54.6, 46.1, 41.0, 28.5, 14.8, 9.0; DEPT spectrum: quaternary carbons  $\delta$  154.6, 139.3, 138.9, 126.3, 124.3; CH carbons  $\delta$  125.7, 123.5, 119.8, 54.6, 46.1; CH<sub>2</sub> carbons  $\delta$  61.6, 41.0, 28.5; CH<sub>3</sub> carbons  $\delta$  14.8, 9.0; IR (drifts) 3350 (s), 3293 (m), 2972 (s), 1697 (vs); MS (ES+) *m/z* (rel intens) 358 (M + H + CH<sub>3</sub>CN<sup>+</sup>, 55), 317 (M + H<sup>+</sup>, 7), 300 (100); Anal. Calcd for C<sub>15</sub>H<sub>19</sub>N<sub>2</sub>O<sub>2</sub>F<sub>3</sub>: C, 56.96; H, 6.06; N, 8.86. Found: C, 56.86; H, 6.28; N, 8.82.

**(-)-(2R,4S)-4-Amino-2-ethyl-6-trifluoromethyl-3,4-dihydro-2H-quinoline-1-carboxylic Acid Ethyl Ester Hemidibenzoyl-L-tartrate Salt (12).** A 1-L flask under nitrogen atmosphere was charged with **11** (24.0 g, 75.9 mmol, 1.0 equiv) and (-) dibenzoyl-L-tartaric acid (anhydrous) (27.19 g, 75.9 mmol, 1.0 equiv). Ethanol (300 mL of  $\sim$ 97%, prepared by adding 10.5 mL of H<sub>2</sub>O to 500 mL of absolute ethanol, mixing, and measuring out 300 mL) was added. The mixture was stirred at room temperature for 18 h and then filtered. The solids were washed 1  $\times$  48 mL of  $\sim$ 97% ethanol and dried to give **12** as a white crystalline solid (14.77 g, 39%): mp 189.5–191.5 °C dec; <sup>1</sup>H NMR (DMSO-*d*<sub>6</sub>, 400 MHz)  $\delta$  0.62 (t, 3H, *J* = 7.3 Hz), 1.16 (t, 3H, *J* = 7.1 Hz), 1.3 (m, 3H), 2.5 (m, 1H), 4.1 (m, 4H), 5.63 (s, 1H, methine proton in DBTA), 7.47 (m, 2H, DBTA aromatic H's), 7.6 (m, 3H, DBTA aromatic H's), 7.68 (s, 1H), 7.95 (m, 2H), 8.2 (br s, NH<sub>3</sub><sup>+</sup>, did not integrate); <sup>13</sup>C NMR (DMSO-*d*<sub>6</sub>, 100 MHz)  $\delta$  169.8, 165.5, 154.1, 140.1, 134.5, 133.5, 130.7, 129.6, 128.9, 126.7, 124.8 (q, *J* = 31.7 Hz), 124.6 (q, *J* = 27.1 Hz), 124.5, 120.9, 74.4, 62.1, 53.5, 45.9, 38.8, 28.2, 14.6, 9.5; DEPT spectrum: quaternary carbons  $\delta$  169.8, 165.5, 154.1, 140.1, 134.5, 130.7, 124.8, 124.6; CH carbons  $\delta$  133.5, 129.6, 128.9, 126.7, 124.5, 120.9, 74.4, 53.5, 45.9; CH<sub>2</sub> carbons  $\delta$  62.1, 38.8, 28.2; CH<sub>3</sub> carbons  $\delta$  14.6, 9.5; IR (drifts) 3278 (m), 2400–3100 (broad), 1703 (vs); MS (ES+) *m/z* (rel intens) 358 (M + H + CH<sub>3</sub>CN<sup>+</sup>, 55), 317 (M + H<sup>+</sup>, 7), 300 (100); Anal. Calcd for C<sub>15</sub>H<sub>19</sub>N<sub>2</sub>O<sub>2</sub>F<sub>3</sub>·C<sub>9</sub>H<sub>7</sub>O<sub>4</sub>: C, 58.18; H, 5.29; N, 5.65. Found: C, 57.99; H, 5.15; N, 5.64; Chiral HPLC: mobile phase 950:50:2 *n*-hexane/2-propanol/HOAc, flow rate 1.50 mL/min, column temp 40 °C, Chiralpak AD 4.6 mm  $\times$  250 mm, sample concentration  $\sim$ 0.5 mg/mL in  $\sim$ 1:1 *n*-hexane/2-propanol. Retention times: 7.5 min 99% (2R,4S) and 10.0 min 1% (2S,4R). [ $\alpha$ ]<sub>D</sub> = -153 (*c* = 1.07, CH<sub>3</sub>OH).

**(-)-(2R,4S)-4-(3,5-Bis-trifluoromethyl-benzylamino)-2-ethyl-6-trifluoromethyl-3,4-dihydro-2H-quinoline-1-carboxylic Acid Ethyl Ester Tosylate Salt (14).** **12** (13.0 g, 26.2 mmol, 1.0 equiv) was suspended in 1,2-dichloroethane (260 mL) in a 500-mL separatory funnel. The mixture was washed 1  $\times$  65 mL of 1 N NaOH, 1  $\times$  65 mL of brine, and

dried (MgSO<sub>4</sub>). The mixture was filtered, concentrated to ~80 mL, and transferred to a 250-mL three-neck flask. **13** (4.53 mL, 27.5 mmol, 1.05 equiv) was added, and the mixture stirred 1 h at room temperature under nitrogen atmosphere. Sodium triacetoxyborohydride (11.1 g, 52.4 mmol, 2.0 equiv) was added in one portion, and the white slurry stirred 18 h. To the slurry were added 50 mL of 1,2-dichloroethane and 50 mL of 2 N NaOH, and the aqueous layer was extracted 2 × 50 mL of 1,2-dichloroethane. The combined organic extracts were washed 1 × 31 mL of 1 N HCl, 1 × 50 mL of saturated aq NaHCO<sub>3</sub>, 1 × 50 mL of brine, and dried (Na<sub>2</sub>SO<sub>4</sub>). The mixture was filtered and concentrated to a clear oil. The oil was dissolved in methanol (71 mL). *p*-Toluenesulfonic acid monohydrate (5.23 g, 27.5 mmol, 1.05 equiv) was added. After 5 min, 284 mL of isopropyl ether was added.<sup>21</sup> The solution was concentrated to ~35 mL, transferred to a 500 mL three neck flask (mech. stirrer), and diluted with 284 mL isopropyl ether. A thick white slurry formed in 10 min. After stirring 3 h, the slurry was filtered and the cake washed 2 × 70 mL of isopropyl ether. After drying, **14** was isolated as a white powder (16.18 g, 86% overall): mp 191–192 °C; <sup>1</sup>H NMR (DMSO-*d*<sub>6</sub>, 400 MHz) δ 0.78 (t, 3H, *J* = 7.5 Hz), 1.21 (t, 3H, *J* = 7.0 Hz), 1.5 (m, 3H), 2.24 (s, 3H), 3.08 (m, 1H), 4.17 (m, 2H), 4.41 (m, 1H), 4.50 (m, 2H), 4.79 (m, 1H), 7.04 (d, 2H, *J* = 7.9 Hz), 7.42 (d, 2H, *J* = 7.9 Hz), 7.7 (m, 2H), 7.81 (s, 1H), 8.21 (s, 1H), 8.35 (s, 2H), 9.58 (br s, 1H), 9.83 (br s, 1H); <sup>13</sup>C NMR (DMSO-*d*<sub>6</sub>, 100 MHz) δ 154.0, 145.4, 140.2, 138.3, 135.3, 132.5, 131.6, 130.7 (q, *J* = 33.2 Hz), 128.4, 127.4, 125.8, 125.3, 124.9 (q, *J* = 31.7 Hz), 124.5 (q, *J* = 27.1 Hz), 123.6 (q, *J* = 27.3 Hz), 123.4, 120.3, 62.3, 53.9, 53.7, 47.9, 33.3, 28.6, 21.1, 14.6, 9.5; DEPT spectrum: quaternary carbons δ 154.0, 145.4, 140.2, 138.3, 135.3, 130.7, 124.9, 124.5, 123.6; CH carbons δ 132.5, 131.6, 128.4, 127.4, 125.8, 125.3, 123.4, 120.3, 53.9, 53.7; CH<sub>2</sub> carbons δ 62.3, 47.98, 33.3, 28.6; CH<sub>3</sub> carbons δ 21.1, 14.6, 9.5; IR (drifts) 2300–3100 (br), 2974 (m), 2731 (m), 2620 (m), 2455 (m), 1714 (s), 1621 (m), 1283 (vs), 1169 (vs), 1126 (vs); MS (ES+) *m/z* (rel intens) 584 (M + H + CH<sub>3</sub>CN<sup>+</sup>, 100), 543 (M + H<sup>+</sup>, 80); Anal. Calcd for C<sub>24</sub>H<sub>23</sub>N<sub>2</sub>O<sub>2</sub>F<sub>9</sub>.C<sub>7</sub>H<sub>8</sub>O<sub>3</sub>S: C, 52.11; H, 4.37; N, 3.92. Found: C, 52.15; H, 4.22; N, 3.69; [α]<sub>D</sub> = -77.9 (*c* = 1.05, CH<sub>3</sub>OH).

(-)-(2*R*,4*S*)-4-[(3,5-Bis-trifluoromethyl-benzyl)methoxycarbonylamino]-2-ethyl-6-trifluoromethyl-3,4-dihydro-2*H*-quinoline-1-carboxylic Acid Ethyl Ester Monoethanolate (**1**). Na<sub>2</sub>CO<sub>3</sub> (s) (6.75 g, 63.7 mmol, 3.5 equiv) was added to a room-temperature solution of **14** (13.0 g, 18.2 mmol, 1.0 equiv) in dry THF (130 mL). Methylchloroformate (3.51 mL, 45.5 mmol, 2.5 equiv) was added neat, dropwise over 2 min. After 24 h, the mixture was

concentrated to 65 mL, diluted with 260 mL of ethyl acetate, and transferred to a separatory funnel. The mixture was washed 1 × 90 mL of 1 N HCl (CO<sub>2</sub> evolution), 1 × 90 mL of saturated aq NaHCO<sub>3</sub>, 1 × 90 mL of brine, and dried (MgSO<sub>4</sub>). Filtration and concentration of filtrate afforded a clear oil, which was costripped 3 × 33 mL of 2*B* ethanol. The oil was dissolved in 33 mL of 2*B* ethanol and seeded with a few milligrams of **1**. After stirring 18 h at room temperature, the slurry was filtered and dried to give **1** monoethanolate as a white crystalline powder (8.66 g, 74%): mp 54–58 °C; <sup>1</sup>H NMR (CDCl<sub>3</sub>, 400 MHz, 55 °C) δ 0.73 (t, 3H, *J* = 7.0 Hz), 1.20 (t, EtOH), 1.27 (t, 3H, *J* = 7.1 Hz), 1.42 (m, 2H), 1.66 (m, 1H), 2.25 (br s, 1H), 3.67 (q, EtOH), 3.79 (s, 3H), 4.2 (m, 3H), 4.33 (m, 1H), 5.2 (br s, 2H), 7.12 (s, 1H), 7.49 (d, 1H, *J* = 8.3 Hz), 7.57 (d, 1H, *J* = 8.5 Hz), 7.73 (s, 2H), 7.78 (s, 1H); <sup>13</sup>C NMR (CDCl<sub>3</sub>, 400 MHz) δ 157.7, 154.3, 141.7, 140.0, 133.8, 132.1 (q, *J* = 33 Hz), 126.9, 124.4, 123.9 (q, *J* = 27.3 Hz), 123.1 (q, *J* = 27.3 Hz), 121.3, 119.1, 62.2, 58.2, 54.4, 53.71, 53.0, 46.6, 37.0, 29.0, 18.2, 14.3, 9.2, (note: the fourth quartet appears to be buried under the δ 126.9 peak, with *J* ≈ 32 Hz); DEPT spectrum: quaternary carbons δ 157.7, 154.3, 141.7, 140.0, 133.8, 132.1, 123.9, 123.1; CH carbons δ 126.9, 124.4, 121.3, 119.1, 54.4, 53.0; CH<sub>2</sub> carbons δ 62.2, 58.2, 46.6, 37.0, 29.0; CH<sub>3</sub> carbons δ 53.7, 18.2, 14.3, 9.2; IR (drifts) 3489 (s), 2974 (s), 2884 (m), 1701 (vs), 1280 (vs), 1131 (vs); MS (ES+) *m/z* (rel intens) 601 (M + H<sup>+</sup>, 100); Anal. Calcd for C<sub>26</sub>H<sub>25</sub>N<sub>2</sub>O<sub>4</sub>F<sub>9</sub>.C<sub>2</sub>H<sub>6</sub>O: C, 52.01; H, 4.83; N, 4.33. Found: C, 51.84; H, 4.54; N, 4.33; chiral HPLC: mobile phase 95:0:5 2*n*-hexane/2-propanol/HOAc, flow rate 1.0 mL/min, 254 nm, Chiralpak AD 4.6 mm × 250 mm, column temp 40 °C, sample concentration ~0.5 mg/mL in 90:10 *n*-hexane/2-propanol, authentic racemate retention times 3.6 and 4.6 min. (-)-(2*R*,4*S*)-4-[(3,5-Bis-trifluoromethyl-benzyl)methoxycarbonylamino]-2-ethyl-6-trifluoromethyl-3,4-dihydro-2*H*-quinoline-1-carboxylic acid ethyl ester monoethanolate shows 4.6 min, 99.1% and 3.6 min, not detected; [α]<sub>D</sub> = -93.3 (*c* = 1.08, CH<sub>3</sub>OH).

#### Acknowledgment

We thank Jon Bordner for the X-ray crystallographic structure determination. We also thank Keith Devries, Jerry Murry, and Steve Ley for helpful chemistry discussions.

#### Supporting Information Available

Computational data and X-ray crystallographic data. This material is available free of charge via the Internet at <http://pubs.acs.org>.

Received for review January 13, 2006.

OP060014A

(21) Any use of isopropyl ether can be hazardous. Please use with caution. See Laird, T. *Org. Process Res. Dev.* **2006**, *8*, 815.